# Observation of $e^+e^- \to \gamma X(3872)$ at BESIII

Yumo Su

May. 19th ,2017

# Outline

Motivation

Reconstruction

Some distributions of observable quantity in data

Fit

Results

# Motivation

- Until now, the $X(3872)$ was only observed in B meson decays and hadron collisions. Since the $X(3872)$ is $1^{++}$ state, it should be able to be produced through the radiative transition of an excited vector charmonium or charmoniumlike states such as a $\varphi$ or Y.

# Reconstruction

tection efficiency, and estimate backgrounds. For the signal process, we generate $e^+e^- \to \gamma X(3872)$, with $X(3872) \to \pi^+\pi^- J/\psi$ at each CM energy. Initial state radiation (ISR) is simulated with KKMC [19], where the Born cross section of $e^+e^- \to \gamma X(3872)$ between 3.90 and 4.42 GeV is assumed to follow the $e^+e^- \to \pi^+\pi^- J/\psi$ line-shape [11]. The maximum ISR photon energy corresponds to the 3.9 GeV/$c^2$ production threshold of the $\gamma X(3872)$ system. We generate $X(3872) \to \rho^0 J/\psi$ MC events with $\rho^0 \to \pi^+\pi^-$ to model the $\pi^+\pi^-$ system and determine the detection efficiency [9]. Here the $\rho^0$ and $J/\psi$ are assumed to be in a relative $S$-wave. Final State Radiation (FSR) is handled with PHOTOS [20].

$e^+e^- \to X(3872) \quad \gamma$

$\downarrow$

$J/\varphi \quad \pi^+\pi^-$

$\downarrow$

$e^+e^-$ or $\mu^+\mu^-$

# Some distributions of observable quantity in data

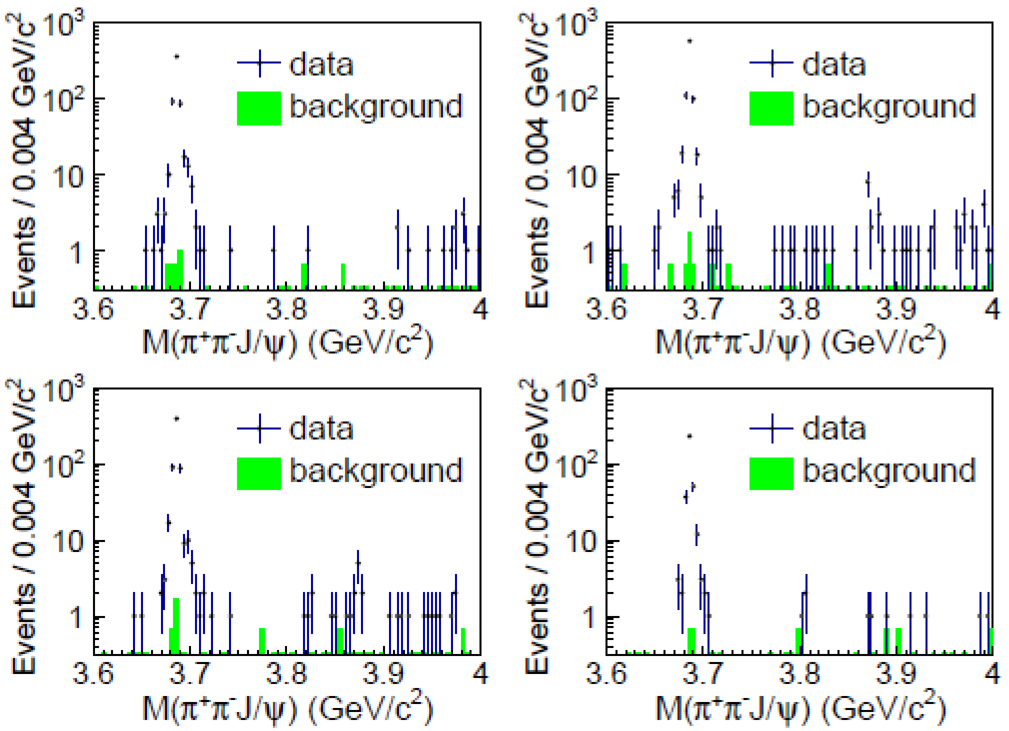


FIG. 1: The $\pi^+\pi^- J/\psi$ invariant mass distributions at $\sqrt{s}$ = 4.009 (top left), 4.229 (top right), 4.260 (bottom left), and 4.360 GeV (bottom right). Dots with error bars are data, the green shaded histograms are normalized $J/\psi$ sideband events.

$M(\pi^+\pi^- J/\psi) = M(\pi^+\pi^-\ell^+\ell^-) - M(\ell^+\ell^-) + m(J/\psi)$ is used to reduce the resolution effect of the lepton pairs, and $m(J/\psi)$ is the nominal mass of $J/\psi$ [13]. There is a huge $e^+e^- \rightarrow \gamma_{\mathrm{ISR}}\psi(3686)$ signal at each CM energy data set. In addition, there is a narrow peak around 3872 MeV/$c^2$ in the 4.229 and 4.260 GeV data samples, while there is no significant signal at the other energies.

# Fit

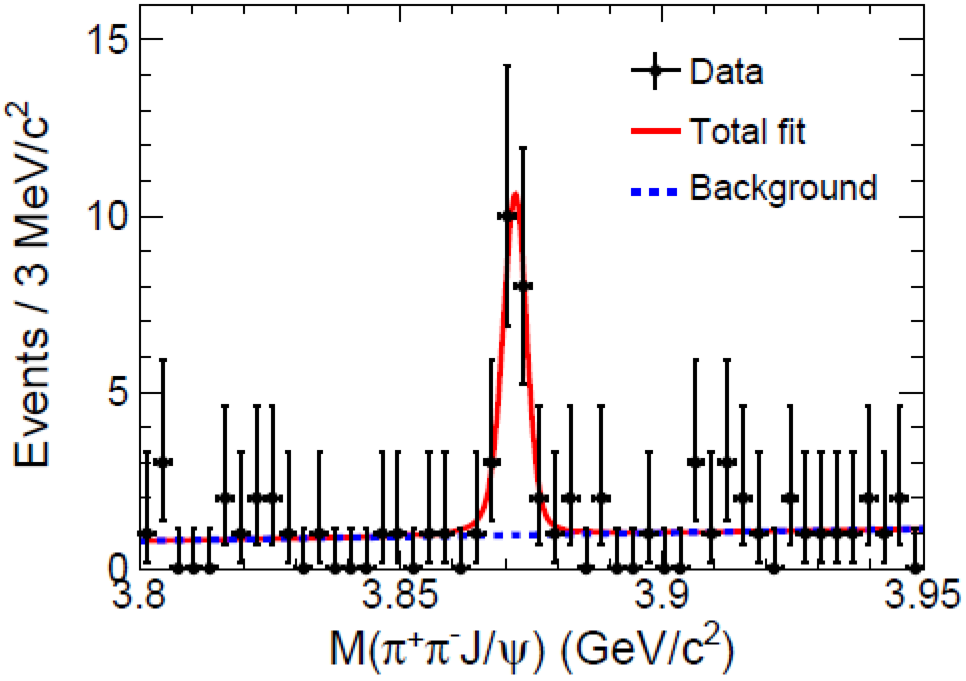


FIG. 2: Fit of the $M(\pi^+\pi^- J/\psi)$ distribution with a MC simulated histogram convolved with a Gaussian function for signal and a linear background function. Dots with error bars are data, the red curve shows the total fit result, while the blue dashed curve shows the background contribution.

The $M(\pi^+\pi^- J/\psi)$ distribution (summed over all CM energy data sets) is fitted to determine the mass and $X(3872)$ yield. We use a MC simulated signal histogram convolved with a Gaussian function which represents the resolution difference between data and MC simulation as the signal shape, and a linear function for the background. The ISR $\psi(3686)$

# Results

TABLE I: The number of $X(3872)$ events ($N^{\rm obs}$), radiative correction factor $(1+\delta)$, detection efficiency ($\epsilon$), measured Born cross section $\sigma^B[e^+e^- \to \gamma X(3872)]$ times $\mathcal{B}[X(3872) \to \pi^+\pi^- J/\psi]$ ($\sigma^B \cdot \mathcal{B}$, where the first uncertainties are statistical and the second systematic), measured ISR $\psi(3686)$ cross section ($\sigma^{\rm ISR}$, where the first uncertainties are statistical and the second systematic), and predicted ISR $\psi(3686)$ cross section ($\sigma^{\rm QED}$ with uncertainties from resonant parameters) from QED [23] using resonant parameters in PDG [13] as input at different energies. For 4.009 GeV and 4.360 GeV, the upper limits of observed events ($N^{\rm up}$) and cross section times branching fraction ($\sigma^{\rm up} \cdot \mathcal{B}$) are given at the 90% C.L.

| $\sqrt{s}$ (GeV) | $N^{\rm obs}$ | $N^{\rm up}$ | $\epsilon$ (%) | $1+\delta$ | $\sigma^B \cdot \mathcal{B}$ (pb) | $\sigma^{\rm up} \cdot \mathcal{B}$ (pb) | $\sigma^{\rm ISR}$ (pb) | $\sigma^{\rm QED}$ (pb) |
|---|---|---|---|---|---|---|---|---|
| 4.009 | $0.0 \pm 0.5$ | $< 1.4$ | 28.7 | 0.861 | $0.00 \pm 0.04 \pm 0.01$ | $< 0.11$ | $719 \pm 30 \pm 47$ | $735 \pm 13$ |
| 4.229 | $9.6 \pm 3.1$ | - | 34.4 | 0.799 | $0.27 \pm 0.09 \pm 0.02$ | - | $404 \pm 14 \pm 27$ | $408 \pm 7$ |
| 4.260 | $8.7 \pm 3.0$ | - | 33.1 | 0.814 | $0.33 \pm 0.12 \pm 0.02$ | - | $378 \pm 16 \pm 25$ | $382 \pm 7$ |
| 4.360 | $1.7 \pm 1.4$ | $< 5.1$ | 23.2 | 1.023 | $0.11 \pm 0.09 \pm 0.01$ | $< 0.36$ | $308 \pm 17 \pm 20$ | $316 \pm 5$ |